Article

Effect of Rubidium on Solidification Parameters, Structure and Operational Characteristics of Eutectic Al-Si Alloy

Igor A. Petrov [1] , **Anastasiya D. Shlyaptseva** [1] , **Alexandr P. Ryakhovsky** [1] , **Elena V. Medvedeva** [2] **and Victor V. Tcherdyntsev** [3,*]

[1] Moscow Aviation Institute, Orshanskaya 3, 125993 Moscow, Russia; petrovia2@mai.ru (I.A.P.); shlyaptsevaad@mai.ru (A.D.S.); ryahovskiyap@mai.ru (A.P.R.)
[2] Institute of Electrophysics, Ural Branch, Russian Academy of Science, Amudsena Str., 106, 620016 Yekaterinburg, Russia; lena@iep.uran.ru
[3] Laboratory of Functional Polymer Materials, National University of Science and Technology "MISIS", Leninskii prosp, 4, 119049 Moscow, Russia
* Correspondence: vvch@misis.ru; Tel.: +7-9104002369

Abstract: Modification of the eutectic silicon in Al–Si alloys causes a structural transformation of the silicon phase from a needle-like to a fine fibrous morphology and is carried out extensively in the industry to improve mechanical properties of the alloys. The theories and mechanisms explaining the eutectic modification in Al–Si alloys are considered. We discuss the mechanism of eutectic rubidium modification in the light of experimental data obtained via quantitative X-ray spectral microanalysis and thermal analysis. X-ray mapping revealed that rubidium, which theoretically satisfies the adsorption mechanisms of silicon modification, had an effect on the silicon growth during solidification. Rubidium was distributed relatively homogeneously in the silicon phase. Microstructural studies have shown that rubidium effectively refines eutectic silicon, changing its morphology. Modification with rubidium extends the solidification range due to a decrease in the solidus temperature. The highest level of mechanical properties of the alloy under study was obtained with rubidium content in the range of 0.007–0.01%. We concluded that rubidium may be used as a modifier in Al-Si eutectic and pre-eutectic alloys. The duration of the modifying effect of rubidium in the Al-12wt%Si alloy melt and porosity in the alloy modified with rubidium were evaluated.

Keywords: cast aluminum alloys; modification; rubidium; microstructure; eutectic silicon; solidification process; porosity

1. Introduction

Cast aluminum alloys are used in the automotive and aerospace industries and occupy a special position among structural materials. This is because of the possibility of achieving an optimal combination of basic operational properties (strength, ductility, corrosion resistance, density, etc.) with technological properties, including excellent casting characteristics.

The phase composition, the structural components and the nature of solidification of any cast aluminum alloy are the most important criteria that determine either the operational or technological properties [1].

During the solidification of an alloy, its internal structure is formed, which is one of the determining factors of its operational properties [2]. Solidification is a complex physical and chemical process that can proceed at different rates and under the influence of various external factors. The course of solidification is affected by the physical characteristics of an alloy and the cooling conditions of the casting. Technological factors, such as the temperature of casting the alloy and various types of melt treatment (including modification), significantly affect the solidification process.

In most cases, modification can be considered as the adding of modifying additives into an alloy—elements are added in an amount from 0.001 to 0.3%. Generally, a large number of elements that have a modifying effect on the structure of Al-Si alloys are known.

Modifying elements change the characteristics of the origin, growth and shape of eutectic silicon crystals. Such elements primarily include some alkaline (Na [3–5] and K [6–8]) and alkaline earth metals (Sr [9–11], Ba [12–14] and Ca [12,15,16]). To date, the modifying effect of a number of REMs (Y [12,17], La [18], Ce [19], Sm [20], Eu [21], Ho [22], Er [23,24] and Yb [12,24,25]) on eutectic silicon crystals is known. Such elements are introduced into aluminum alloys with Si content from 6 to 13%, where the eutectic is the main structural component of the alloy. To explain the modification of Al-Si alloys, the theory of supercooling by Edwards and Archer [26] as well as adsorption theories considering the adsorption mechanisms of silicon modification are used. Thus, according to the "Twin plane re-entrant edge" (TPRE) "poisoning" mechanism proposed by Day and Hellawell [27], the modifying element is adsorbed at active growth points in the re-entrant edges of twins, retarding the growth of silicon crystals and changing their growth directions. This deactivates the TPRE mechanism, causing silicon crystals to grow in a more isotropic manner. The basic idea of the "Impurity-induced twinning" (IIT) mechanism proposed by Lu and Hellawell [28] is that the atoms of the modifying element are absorbed on the steps of a growing silicon crystal at the interface between the solid and liquid phases. This leads to the formation of new twins and consequently ensures their growth in other directions. According to the IIT mechanism, only elements showing the "ideal" ratio of atomic radii $r_i/r \sim 1.646$ (where r_i is the atomic radius of the element and r is the radius of silicon) are modifiers.

The interest of researchers in the processes of structure formation during modification of Al-Si alloys has led to the advancement of modification technologies and the production of high-quality castings as well as the development and confirmation of various modification theories.

Of great interest is the use of Rb for modifying Al-Si alloys. There is insufficient literature data on the use of rubidium as a modifier in aluminum–silicon alloys. Rubidium is a chemically active alkali metal with a melting point of 39.3 °C [29]. It is close in its physical and chemical properties to sodium; therefore, it is assumed that the modifying effect of rubidium on a eutectic (α + Si) is similar to the action of sodium. Based on the adsorption theory of modification, the most effective modifiers that refine a eutectic (α + Si) are elements with a low surface tension. Rubidium has a surface tension equal to 83 mN/m [30]. It is significantly lower than the surface tension of aluminum (914 mN/m) and silicon (865 mN/m) [30].

Rubidium has not received practical application in the foundry of eutectic Al-Si alloys. This is due to the complexity of adding this metal into the melt, and the lack of information regarding its effect on the properties of Al-Si alloys. Data on its modifying effect on Al-Si alloys are contradictory [6,28,31]. Rubidium in its pure form is difficult to add to the melt; therefore, it was decided to use salt to add it.

The effect of rubidium on the structure, mechanical properties and solidification of a eutectic Al-Si alloy was examined in our study. The duration of the modifying effect of rubidium in the Al-Si alloy melt was determined, and the porosity of an alloy modified with rubidium was evaluated.

2. Materials and Methods

2.1. Materials and Modification Technology

The object of the study was a eutectic Al-12wt%Si alloy. The chemical compositions of the experimental alloys are presented in Table 1.

Table 1. Chemical compositions of experimental alloys.

Al-12wt%Si Alloy	Estimated Quantities Rb %	Mass Fraction, % (Al-Base)						
		Si	Cu	Mn	Ti	Zn	Fe	Rb
Unmodified	—	11.42	0.0020	0.002	0.007	0.0097	0.22	—
Alloy 1	0.1	11.39	0.0017	0.0023	0.004	0.0090	0.22	0.002
Alloy 2	0.3	11.51	0.0013	0.002	0.006	0.01	0.26	0.0052
Alloy 3	0.5	11.36	0.0021	0.0026	0.006	0.0092	0.20	0.0075
Alloy 4	1.0	11.48	0.0018	0.0042	0.009	0.01	0.25	0.01

Salt ($RbNO_3$) was chosen as the compound to add rubidium into the melt. The estimated amounts of rubidium added to the alloy were chosen to be equal to 0.1%, 0.3%, 0.5%, and 1.0% from the weight of the melt. The salt was dried at 150–200 °C for 2 h before melting.

Experimental melting was carried out in an electric resistance furnace. The weight of one melt was 1 kg. The melt was previously degassed with argon. Rubidium salt ($RbNO_3$) was added into the melt at the bottom of the crucible at a temperature of $750 \pm 5°$ with the help of a "bell". The treatment of the melt with the salt was accompanied by bubbling. Then, the melt stood for 10 min, slag was removed from its surface, and samples of the experimental alloys were poured into a sandy-clay mold at a temperature equal to 710 ± 5 °C. Samples were cast separately to determine porosity.

The weight of the melt to determine the duration of the modification effect was equal to 5 kg. The melt was kept at a constant temperature equal to $730 \pm 5°$C for up to 240 min. In the process of holding the melt, samples were poured into a sandy-clay mold at the time intervals of 15, 30, 45, 60, 120, 180 and 240 min.

2.2. Methods of Studying the Microstructure and Mechanical Properties

The mechanical properties of the experimental alloys (ultimate strength and relative elongation) were determined in accordance with ASTM B557M-15 on an Instron 5982 testing machine (Instron, Norwood, MA, USA). In each experiment, 4 samples were tested. Each experiment was repeated twice.

Microstructural studies were carried out on a Carl Zeiss-brand Imager.Z2m AXIO universal research motorized microscope (Carl Zeiss, Microscopy GmbH, Göttingen, Germany).

Quantitative analysis of the microstructure (average length, area of eutectic silicon and α-Al dendrites) was carried out using the specialized program ImageExpert Pro 3.7, version 3.7.5.0, NEXSYS, (Moscow, Russia) over three images per each sample. The photographs were processed through the use of the following operations: changing the size of the photograph, selecting the scale, binarization, determining the object of study by color, etc. For image processing, the ImageExpert Pro 3.7 program uses built-in algorithms (the methods correspond to the ASTM E112-10 international standard).

To measure the size of the α-Al dendrite, the secondary dendrite arm spacing (SDAS) was determined. The SDAS was evaluated (as reported in [32]) by measuring thirty dendrites for each sample using three images at $50\times$ magnification.

The microstructure and elemental composition and distribution of modifying elements in the structure were studied using a Phenom XL scanning electron microscope (SEM) with an integrated energy-dispersive spectrometry (EDS) system (Phenom-World BV, Eindhoven, Netherlands). To determine the elemental composition at a point and according to area, the method of quantitative X-ray spectral microanalysis was used using special Phenom Element Identification v. 3.8.0.0 software. To carry out X-ray mapping, the Elemental Mapping software was used.

2.3. Methods of Chemical and Thermal Analysis

The chemical (elemental) composition of the samples was studied using a CCD-based Q4 TASMAN-170 spark optical emission spectrometer. The Q4 TASMAN-170 spectrometer was controlled from a desktop computer using special QMatrix software version 3.8.1 (Bruker Quantron GmbH, Kalkar, Germany).

The actual rubidium content was obtained using an ICAP 6300 inductively coupled plasma atomic emission spectrometer (ICP-AES) (Thermo Fisher Corporation, Cambridge, UK).

Thermal analysis of the alloys' solidification was carried out using a Netzsch DSC404 F3 Pegasus differential scanning calorimeter (Netzsch-Geratebau GmbH, Bavaria, Germany). The samples were subjected to exposure at room temperature for 24 h before the test. The analyzed sample and the platinum standard were placed with thermocouples (Pt–Rh) in platinum crucibles and put into the heating chamber of the installation. The tests were carried out in an inert argon atmosphere. NETZSCH Proteus$^{\circledR}$ v. 7.1 software was used to process the data obtained (Netzsch-Geratebau GmbH, Bavaria, Germany).

2.4. Porosity Investigation Method

The porosity of the alloys was evaluated on a five-level standard scale in macrosections of samples cut from castings in sandy-clay molds in accordance with ISO 10049:2019(E) [33]. To disclose the pores, the sample was sanded and etched in a 20% NaOH solution in accordance with ISO 10049:2019(E).

3. Results

3.1. Thermodynamic Analysis of the Interaction of Rubidium Nitrate with Melt

The study of an alloy modification with rubidium using $RbNO_3$ salt is impossible without a preliminary thermodynamic analysis. In this regard, the thermodynamic probability of the salt-decomposition process and its interaction with the melt up to a temperature of 1200 K (927 °C) was determined. Calculations of the free reaction energy were carried out while taking into account phase transformations based on the literature data [34,35].

It is known [34] that rubidium nitrate $RbNO_3$ is a low-melting salt (melting point t = 313 °C) and that when heated above the melting point, it decomposes to form a nitrite and oxygen according to Reaction (1):

$$RbNO_3 = RbNO_2 + 0.5O_2 \tag{1}$$

The resulting $RbNO_2$ reacts with aluminum and is reduced to rubidium according to Reaction (2):

$$RbNO_2 + \frac{4}{3}Al = \frac{2}{3}Al_2O_3 + \frac{1}{2}N_2 + Rb \tag{2}$$
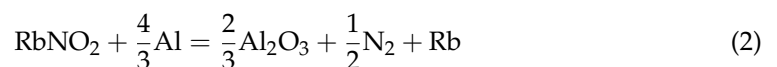
At the same time, direct interaction of the nitrate with aluminum according to Reaction (3) with the formation of rubidium is also possible:

$$RbNO_3 + 2Al = Al_2O_3 + \frac{1}{2}N_2 + Rb \tag{3}$$
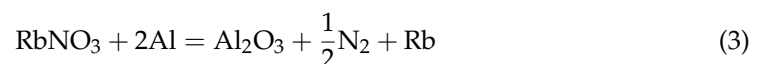
According to the calculations obtained, the free reaction energy for Reactions (2) and (3) at the temperatures of 600–1200 K was negative (Figure 1). Consequently, at the salt input temperature of 1023 K (750 °C), the formation of rubidium in the aluminum melt was possible according to Reactions (2) and (3), for which the energy of the system reached values of −432 and −367 kJ/mol, respectively.
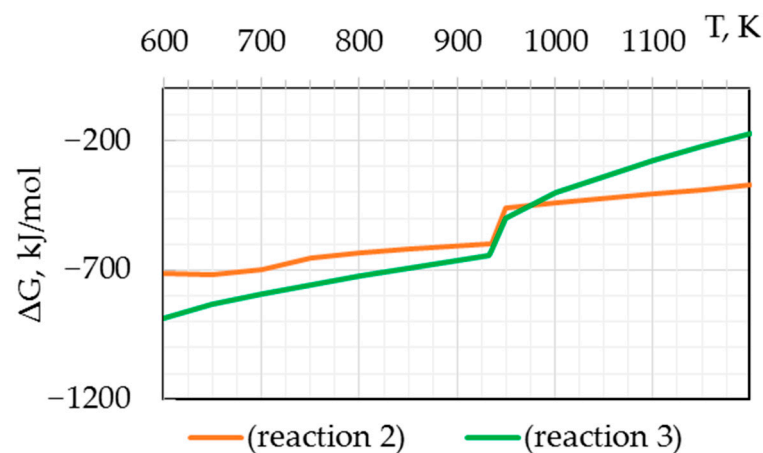
Figure 1. Temperature dependences of the free reaction energy of Reactions (2) and (3) on temperature.

3.2. Mechanical Properties

The results of mechanical tests of the Al-12wt%Si alloy after modification with rubidium are presented in Table 2. It was experimentally established that adding rubidium caused an increase in the mechanical properties (ultimate strength σ_B and relative elongation δ).

Table 2. Mechanical properties of Al-12wt%Si alloy and average dimensions of eutectic Si and SDAS.

Al-12wt%Si Alloy	Features			
	σ_v, MPa	δ, %	l_{Si} eut, μm	SDAS, μm
Unmodified	145 ± 2	2.6 ± 0.2	$14 - 49.4$	42 ± 10
Alloy 1	149 ± 2	4.1 ± 0.1	$5.42 - 28.58$	40 ± 9
Alloy 2	166 ± 3	5.5 ± 0.4	$\frac{1.88 - 7.88}{0.7 - 22}$	37 ± 10
Alloy 3	169 ± 1	9.3 ± 0.5	$\frac{0.36 - 2.29}{0.2 - 7.6}$	37 ± 9
Alloy 4	171 ± 2	8.6 ± 0.5	$\frac{0.72 - 3.97}{0.29 - 11.7}$	39 ± 8

Note: the numerator shows the average size of the structural components and the denominator shows the minimum and maximum size.

The largest increase in the mechanical properties of the alloy 3 is explained by the modified microstructure of the alloy. An increase in the Rb content in alloy 4 did not lead to a further increase in mechanical properties, which remained at the level of alloy 3.

3.3. Microstructural Studies

The results of the optical microscopy of the structures of the unmodified Al-12wt%Si alloy and those modified with different rubidium content are shown in Figure 2. For alloy 3, the results of the X-ray spectral microanalysis and EDS elementary mapping are presented in Figure 3.

In the Al-12wt%Si alloy under study, the silicon concentration was 11.4%. The microstructure of the unmodified alloy was characterized as coarse eutectic (l_{Si} eut = 14–49.4 μm) with large α-Al dendrites (SDAS 42 μm). Due to the presence of impurities and low cooling rates (casting into a sandy-clay mold), primary silicon crystals could be observed in the structure of the alloy under study. The iron concentration in the alloy was about 0.3%, which can lead to the β-FeSiAl$_5$ phase formation.
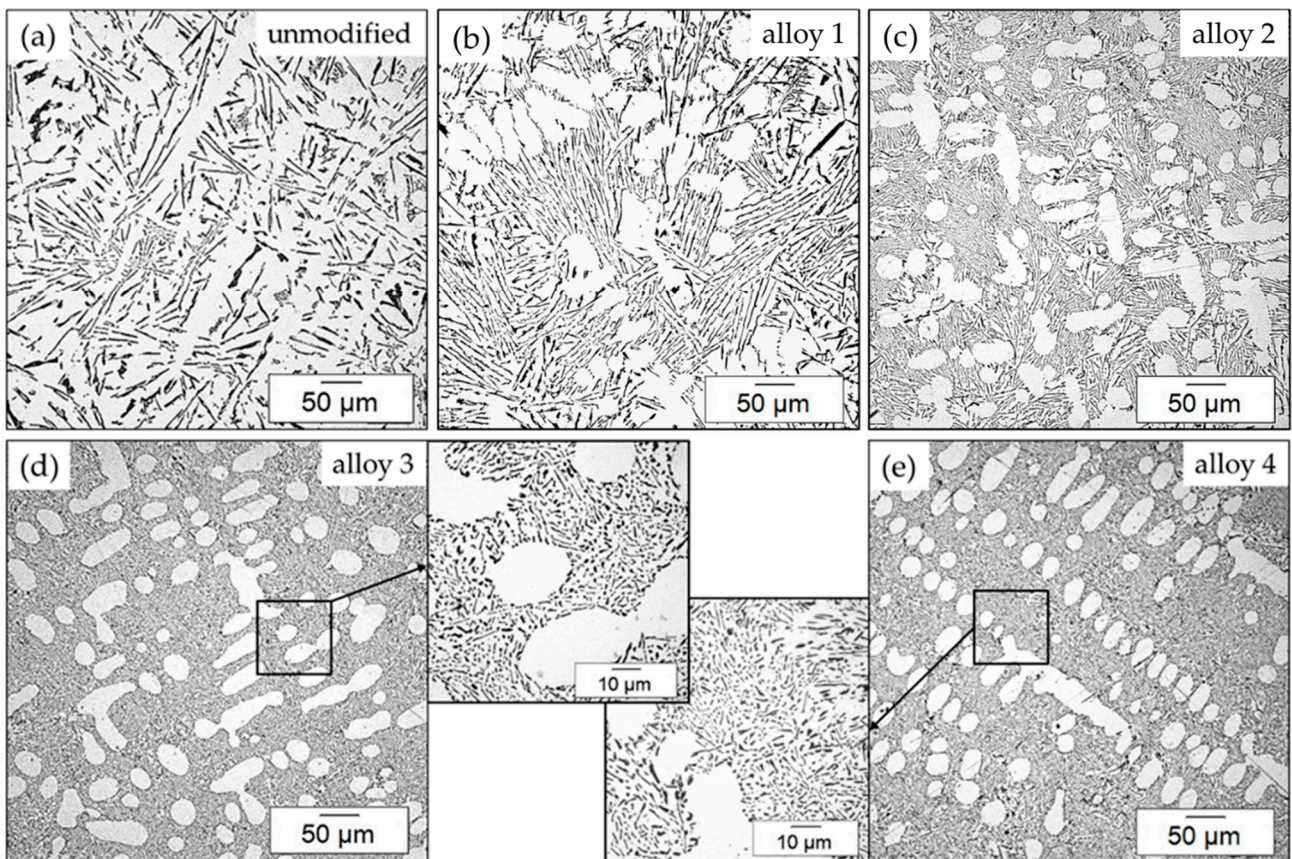
Figure 2. Microstructure of Al-12wt%Si alloys: (**a**) unmodified; (**b**) alloy 1; (**c**) alloy 2; (**d**) alloy 3; (**e**) alloy 4.

Element Symbol	Atomic Conc.	Weight Conc.
Al	88.35	87.39
Si	11.32	11.66
Rb	0.24	0.75
Fe	0.09	0.19

Element Symbol	Atomic Conc.	Weight Conc.
Al	87.60	86.86
Si	12.20	12.60
Rb	0.12	0.37
Fe	0.08	0.17
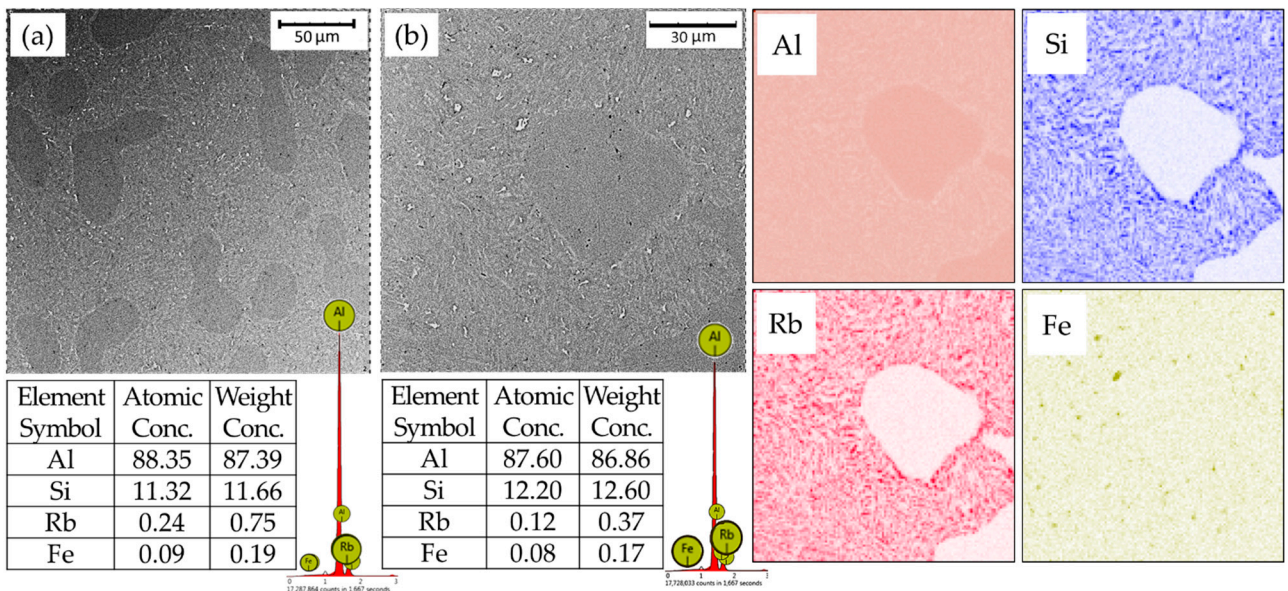
Figure 3. *Cont.*
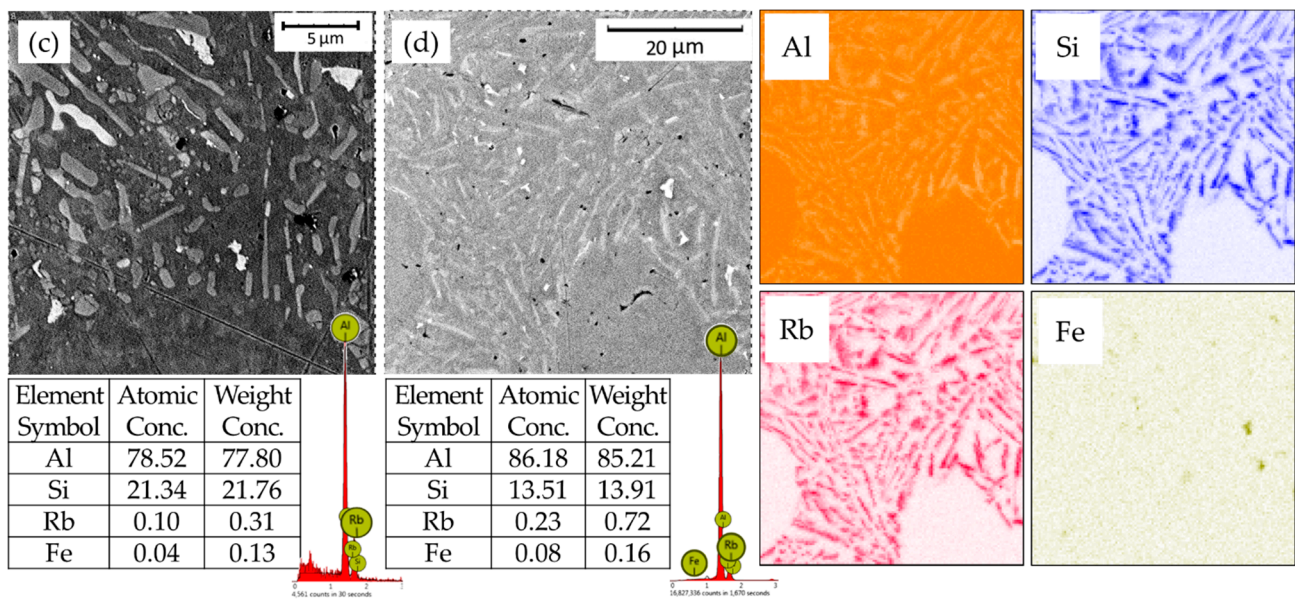
Figure 3. Energy-dispersive X-ray spectral microanalysis of a sample of alloy 3 and elementary mapping of the studied area of a sample modified with rubidium. (**a**) Magnification at 1100× (composition according to area); (**b**) magnification at 2150× (composition according to area and mapping according to elements); (**c**) magnification at 11,500× (composition according to area); (**d**) magnification at 4300× (composition according to area and mapping according to elements).

Studies of the microstructure of alloy 1 showed that modification with a minimal amount of rubidium led to a change in morphology, a decrease in the linear dimensions of the eutectic silicon length to 5.42–22.58 μm, and a decrease in α-Al dendrites by 5%. With an increase in the rubidium content in alloys 2 and 3, the respective linear dimensions of the eutectic silicon decreased to 1.33–5.02 and 0.36–2.29 μm (Table 2). As a result, the Si particles acquired a finer fibrous morphology, as shown in Figure 2d,e. An increase in the rubidium content in alloy 4 did not lead to greater refinement of eutectic silicon (Figure 2d). Different contents of rubidium weakly affected the size of the α-Al dendrites, and the SDAS in the alloy decreased by an average of 11–12%. Therefore, in order to obtain a modified eutectic in the alloy under study, it was necessary to ensure the actual rubidium content in the range of 0.007–0.01 wt %. Therefore, further studies were carried out with an estimated rubidium content of 0.5% (corresponding to 0.0075 wt %).

Based on the results of studying the microstructure of the sample of alloy 3, the presence of rubidium in the studied samples was studied using X-ray spectral microanalysis over the area of the image. The structure, X-ray spectrum and composition of the elements are shown in Figure 3a,c.

To confirm the elemental composition, elementary mapping of a sample of alloy 3 modified with rubidium was carried out. The elementary maps of the rubidium-modified sample in the eutectic area (containing aluminum, silicon and the Fe-containing phase) obtained by scanning at a low resolution are shown in Figure 3b, and a higher-resolution map is shown in Figure 3d. The mapping results showed that rubidium atoms were present in the eutectic silicon and had a low concentration.

3.4. Thermal Analysis

The solidification parameters of the alloys under study (depending on the melt treatment) are presented in Table 3.

Al-12wt%Si,	Solidification Parameters, Temperature (°C)			
	Liquidus (t_{liq})	**Solidus (t_{sol})**	**Solidification Range (Δt)**	**Beginning of Solidification of Eutectic ($t_{eu.sol.st}$)**
Unmodified	582.0	557.5	24.2	576.0
Alloy 1	581.0	551.0	30.0	571.9
Alloy 2	581.5	549.1	32.2	570.6
Alloy 3	581.8	539.3	42.5	568.4
Alloy 4	581.7	538.2	43.5	567.9

A DSC curves analysis (Figure 4) showed two-stage solidification of the Al-12wt%Si alloy samples from the liquid state up to complete solidification. In the first stage, the nucleation of aluminum solid solution crystals and their growth occurred, which was recorded in the DSC thermogram as the first thermal effect. The second thermal effect (second stage) was caused by the solidification of the binary eutectic according to the reaction $L \rightarrow \alpha + Si$. Since the alloy contained an iron impurity, during solidification of this alloy, not only the formation of binary eutectic ($\alpha + Si$) was possible but also a more complex iron-containing eutectic $L \rightarrow \alpha + Si + Al_5FeSi$ could form. The solidification temperatures of these eutectics were close [1].
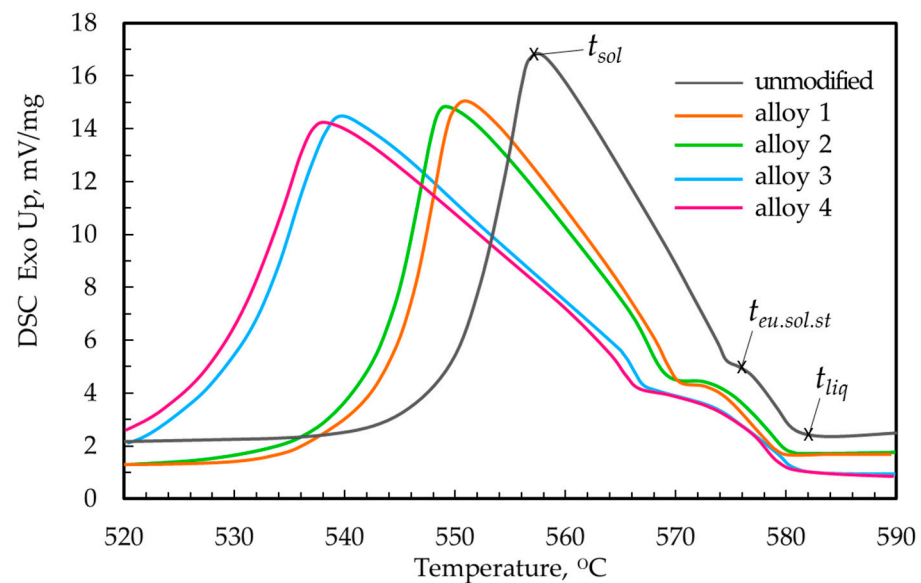
Figure 4. Thermograms of experimental alloys.

In the alloys studied, the solidification parameters changed with an increase in the rubidium concentration. Alloy modification with rubidium decreased the solidus temperatures and the temperatures at which the solidification of the eutectic began compared to the unmodified alloy. As a result, the solidification range of the Al-12wt%Si alloys under study expanded (Table 3). According to the data obtained (Figure 4), the most pronounced change in solidification parameters occurred in alloys 3 and 4.

An analysis of the alloy 3 sample's solidification parameters showed that rubidium did not change the liquidus temperature, which remained at the level of the unmodified alloy, while at the same time the solidus temperature decreased by 18.2 °C. The solidification range of the alloy with rubidium under study expanded by 18.3 °C compared to the unmodified alloy. It should be noted that the temperature of the beginning of the second thermal effect on the alloys was considered as the temperature of the beginning of

solidification of the eutectic (Table 3). Rubidium contributed to a significant decrease in the temperature of the beginning of the solidification of the eutectic (α + Si) compared to the unmodified alloy (equal to 7.6 °C).

3.5. Study of the Effect of Rubidium on the Porosity of the Alloy

A qualitative assessment of the effect of rubidium on the formation of gas porosity in the experimental alloys at different concentrations of rubidium was carried out (Figure 5).
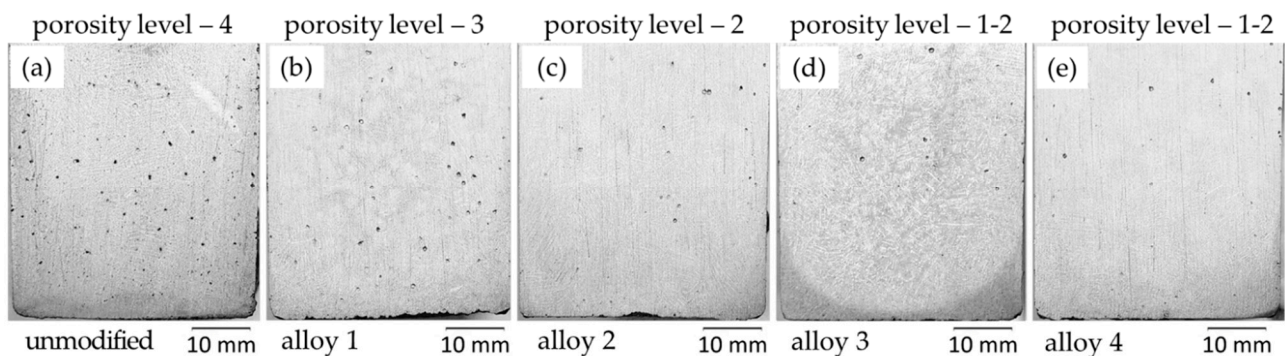
Figure 5. Porosity distribution in Al-12wt%Si alloy castings when modified with rubidium: (**a**) unmodified; (**b**) alloy 1; (**c**) alloy 2; (**d**) alloy 3; (**e**) alloy 4.

The studies showed that the samples of the Al-12wt%Si alloys treated with rubidium had a decrease in gas porosity compared to an unmodified alloy, the porosity of which corresponded to four levels on the standard ISO 10049:2019(E) porosity scale. In alloy 1, the porosity corresponds to level 3, and with an increase in the rubidium content in alloy 4, the porosity decreased to level 1 according to the porosity scale (Figure 5).

Studies were also conducted on the effect of modification of the Al-12wt%Si alloy with rubidium on the manifestation of volumetric shrinkage of the experimental alloys. The formation of shrinkage defects in a massive element, which was the thermal center of the casting, was studied. Since the unmodified Al-12wt%Si alloy had a narrow crystallization interval of 24.2 degrees, it crystallized frontally (successively) (Figure 6a). In this case, a shrinkage cavity was formed on the upper surface of the sample, and the shrinkage porosity was formed on the opposite side. Alloy 3 modified with rubidium had a larger crystallization interval that equaled 42.5 degrees. Therefore, it was more prone to bulk crystallization. At the same time, a shrinkage cavity was formed at the top, and distributed porosity was formed below it (Figure 6b).
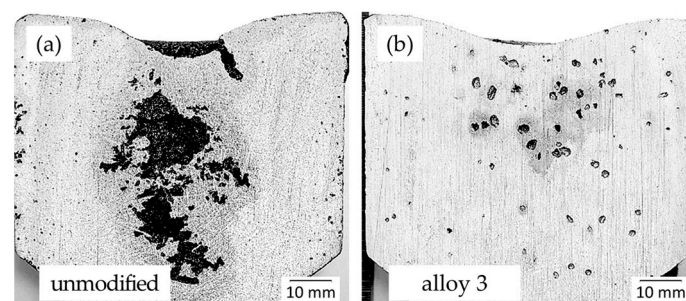
Figure 6. The manifestation of volumetric shrinkage in the Al-12wt%Si alloy: (**a**) unmodified; (**b**) modified with Rb.

3.6. Evaluation of the Duration of the Modifying Effect of Rubidium in the Melt

Based on the studies shown above, alloy 3 was selected to determine the duration of the modifying effect. Treatment of the melt with rubidium led to an increase in the duration of the effect of modifying the Al-Si alloy (Figure 7a,b) compared to sodium modifiers [7].

During the first 30 min after the melt treatment, the σ value of the Al-12wt%Si alloy modified with rubidium was 176 MPa. However, with a longer holding time of up to 60 and 120 min, the ultimate strength of the rubidium-modified alloy decreased slightly to 173 and 170 MPa, respectively. With further holding of the melt up to 240 min, the ultimate strength of the rubidium-modified alloy decreased to 155 MPa.
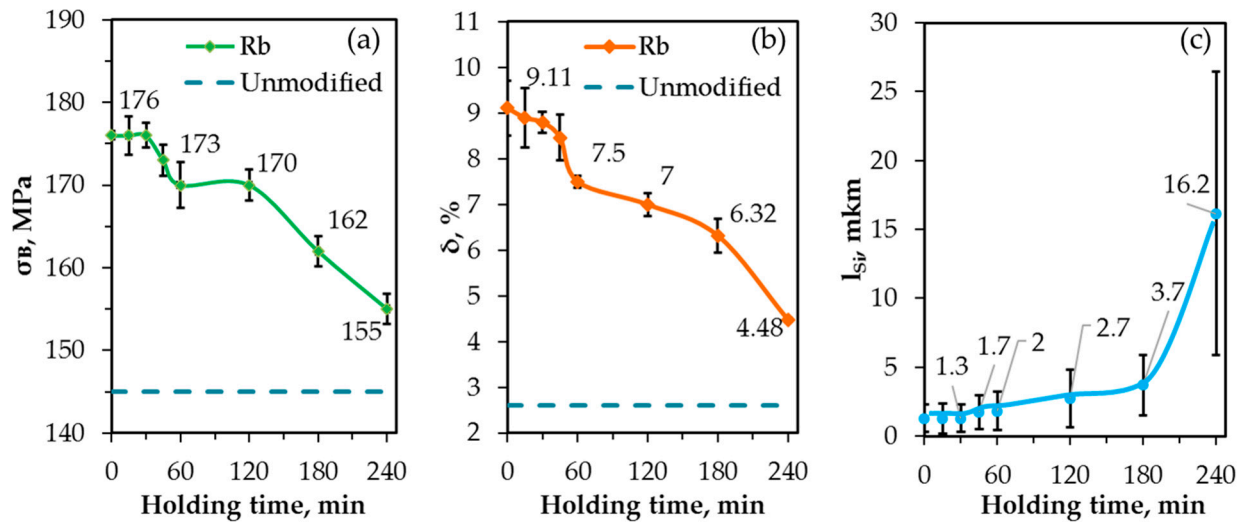
Figure 7. Effect of melt holding time after rubidium modification on: (**a**) ultimate strength; (**b**) relative elongation; (**c**) the average length of eutectic silicon particles.

The values of the relative elongation of the Al-12wt%Si alloy modified with Rb remained at approximately the same level (from 9.1 to 8.46%) during the first 45 min. However, with a longer holding time from 60 to 180 min, the relative elongation of the Al-12wt%Si alloy modified with rubidium decreased from 7.5% to 6.32%.

When holding the melt up to 240 min, the relative elongation of the rubidium-modified alloy decreased significantly to 4.48%.

When modifying the Al-12wt%Si alloy with rubidium, the refined eutectic silicon phase endured for 45 min. A thin fibrous morphology of eutectic silicon was observed (Figure 8a–d). With the increase in the holding time from 60 to 120 min, a smooth size enlargement and coarsening of the eutectic (α + Si) was observed in the microstructure of the alloy (Figure 8e,f). With further holding of the melt up to 180 min, changes to the thin-plate shape in the morphology of the eutectic silicon were observed (Figure 8g). With the proceeding increase in the holding time to 240 min, an abrupt enlargement in size and coarsening of the eutectic (α + Si) was observed in the microstructure of the alloy. The morphology of eutectic silicon changed to needle-like (Figure 8h). However, even with such a long melt holding time, the resulting structure could be characterized as partially modified.

Quantitative analysis of the microstructure of the Al-12wt%Si alloy modified with rubidium showed that an increase in the melt holding time led to an increase in the linear size of the eutectic silicon (Figure 7c). After holding the melt with rubidium modification for 60 min, the average length of eutectic silicon particles increased from 1.3 to 2 microns, after 120 min—to 2.7 microns, and after 180 min—to 3.7 microns. With further exposure of the melt for another 60 min, a sharp increase in the linear sizes of the silicon particles to 16.2 microns occurred.
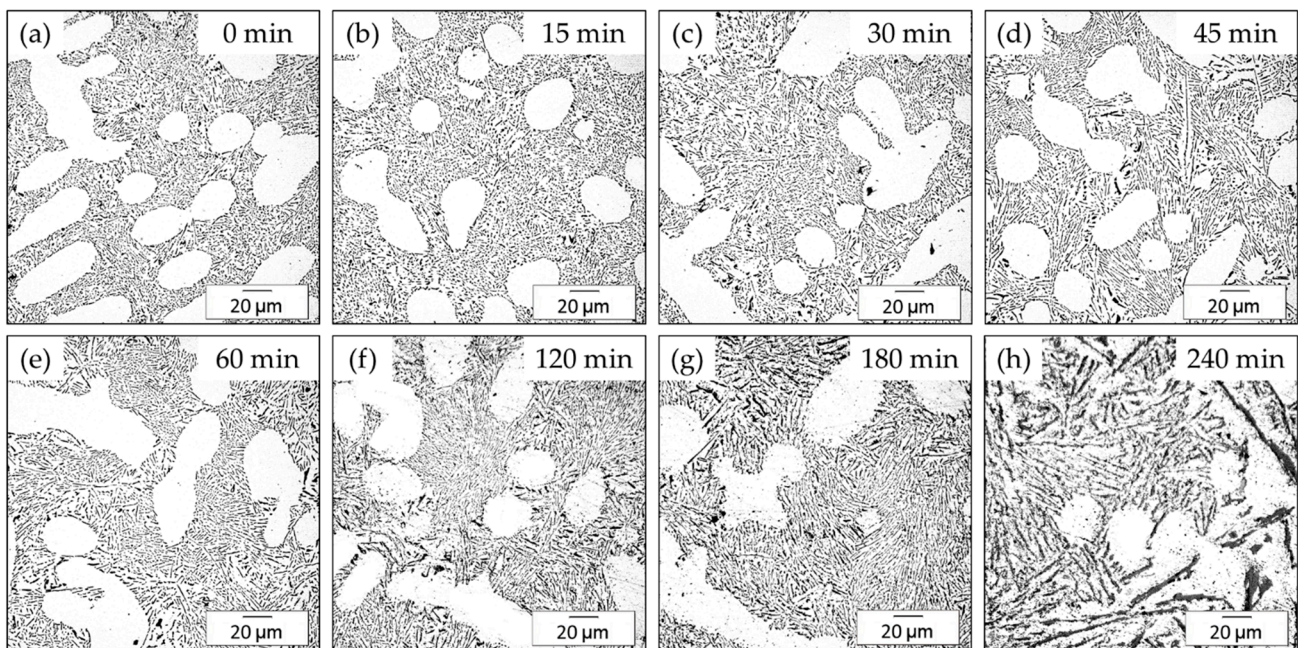
Figure 8. Effect of the melt holding time after modification of the microstructure of alloy 3. (**a**) 0 min.; (**b**) 15 min.; (**c**) 30 min.; (**d**) 45 min.; (**e**) 60 min.; (**f**) 120 min.; (**g**) 180 min.; (**h**) 240 min.

4. Discussion

To determine the possibility of modifying the Al-12wt%Si alloy under study with $RbNO_3$ salt, a thermodynamic analysis of the probable chemical Reactions (2) and (3) was carried out. The formation of rubidium and nitrogen in the melt was thermodynamically possible and confirmed experimentally. During the experimental melting, the release of gaseous compounds during the adding of the salt into the melt was noted.

Based on the obtained data from the atomic emission spectral analysis and energy-dispersive X-ray spectral microanalysis of the samples modified with Rb, it can be concluded that rubidium passed into the melt when added with its nitrate.

The assimilated amount of the modifying element in the range of 0.007–0.01% was sufficient to modify the structure and increase the mechanical properties of the alloy under study.

When modified with rubidium, a thin fibrous eutectic structure was obtained, which is typical of a structure with standard Al-Si alloy modifiers such as sodium and strontium [4,5,36].

The modification mechanism of eutectic silicon by rubidium can be explained using the theory of supercooling and adsorption theory; in particular, the adsorption mechanism of the modification of eutectic silicon.

Firstly, the basis of the theory of supercooling is the data of thermal analysis. According to the theory of supercooling [26], modification of Al-Si alloys lowers the temperature of the beginning of the solidification of the eutectic. An analysis of the DSC thermograms confirmed that rubidium contributed to a significant decrease in the temperature of the beginning of the solidification of the eutectic (α + Si), which led to supercooling of the melt contributed to the appearance of more embryos, and consequently led to the modification of the eutectic.

Secondly, since rubidium is close in its physical and chemical properties to sodium and is a surface-active element, it can be assumed that it will work via a "poisoning" (TPRE) mechanism [27].

On the other hand, according to the IIT mechanism, only elements showing the "ideal" ratio of atomic radii $r_i/r \sim 1.646$ (where r_i is the atomic radius of the element and r is the radius of silicon) are modifiers.

However, rubidium has a ratio of its atomic radii of $r_i/r = 2.08$ [28] and does not meet this criterion, as do some other modifying elements (for example, Sr, Ba and Na). This

indicates that the ratio of the atomic radii of a potential modifying element by itself is not capable of predicting the spheroidization of eutectic silicon.

Thus, besides the atomic radius, other factors that are important for the modification of eutectic silicon (the vapor pressure, the formation of secondary compounds or oxides as well as phase equilibria with aluminum and silicon phases, and the cooling rate) probably exist.

The concept of the "poisoning" mechanism (TPRE) and IIT suggests the formation of a high density of twinning in modified silicon crystals [26,28,37,38]. In order for the impurity rubidium atoms to cause such a high twinning density, it is necessary that they are relatively evenly distributed (at least at the nucleation stage) throughout the silicon crystal, as was observed in the results of the energy-dispersive X-ray spectral microanalysis and elementary mapping in our studies. Thus, these results confirmed the operation of the "poisoning" mechanism (TPRE) and IIT in the rubidium-modified 12wt%Si alloy.

It should be noted that the mechanism of rubidium modification has not yet been fully determined and requires further research.

The observed decrease in gas porosity when modifying the studied alloys with rubidium can be caused by the degassing effect of nitrogen formed during the decomposition of the $RbNO_3$ salt according to Reactions (2) and (3). The hydrogen dissolved in the melt diffused into the floating nitrogen bubbles and was removed from the liquid metal. An increase in the amount of salt added to the melt for its modification led to an increase in the degree of degassing of the 12wt%Si alloy.

The formation of shrinkage defects in a casting is affected by the nature of the solidification of the alloy. Under the same cooling conditions, the main effect on the nature of the solidification of alloys is exerted by the temperature range of solidification. Narrow-interval alloys, which include the 12wt%Si alloy, are characterized by sequential or frontal solidification with slight supercooling and the formation of a concentrated shrink shell [39–41].

With an increase in the solidification range of an alloy, the tendency the alloy to lose porosity increases. It is known that when modifying Al-Si alloys with surfactants, which include rubidium, the degree of supercooling of such alloys increases [40,41]. When modifying the 12wt%Si alloy with rubidium, the liquidus temperature of the alloy practically did not change compared to the unmodified alloy (Table 3). At the same time, as a result of the adsorption of rubidium atoms onto the solidification centers of the eutectic (Figure 3), their deactivation occurred. The solidus temperature of the experimental alloy decreased, and its degree of hypothermia increased. According to the authors of [42,43], due to the neutralization of solidification, eutectic colonies grow in the form of spheroids, forming isolated pores when closing. As a result, volumetric solidification and the formation of shrinkage porosity occurred in the thermal center of the casting (Figure 6b).

The results of the studies conducted to determine the duration of the modifying effect showed that when treated with rubidium, the modifying effect in the melt lasted up to 180 min. This was indirectly confirmed by the mechanical properties and quantitative analysis of the microstructure at different melt holding times. Apparently, the duration of the modifying effect depended on the kinetics of oxidation of rubidium in the melt, which requires additional research. Compared to commonly used eutectic silicon modifiers [44,45], the retention time of the modifying effect of rubidium is higher than that of Na but lower than that of Sr.

5. Conclusions

1. The results of the studies conducted showed that the use of rubidium as a modifier is an interesting direction for improving the structure of cast aluminum alloys and improving their mechanical properties. The most stable and highest level of mechanical properties was obtained via modification with rubidium using an actual content in the range of 0.007–0.01%.
2. Microstructural studies showed that rubidium effectively refined eutectic silicon and changed its morphology but had little effect on α-Al (SDAS) dendrites. Energy-

dispersive X-ray spectral microanalysis and elementary mapping showed the presence of impurity rubidium atoms in modified silicon crystals.

3. Thermal analysis showed that modification with rubidium changed the solidification parameters of the 12wt%Si alloy, causing an extension of the solidification range. The solidus temperature decreased by 18.2 °C. Rubidium contributed to a significant decrease in the temperature of the beginning of the solidification of the eutectic by 7.6 °C.

4. When the 12wt%Si alloy was treated with $RbNO_3$ salt, the melt was degassed and the gas porosity decreased. Modification with rubidium allowed the duration of the modifying effect to be maintained in the melt for up to 180 min.

Conflicts of Interest: The authors declare no conflict of interest.

References

1. Belov, N.A. *Phase Composition of Industrial and Promising Aluminium Alloys: Monograph*; MISiS Publishing House: Moscow, Russia, 2010; 511p.
2. Petrov, I.A.; Shlyaptseva, A.D. Effect of REE on the solidification of eutectic silumin. *Russ. Metall. Met.* **2022**, *3*, 204–210. [CrossRef]
3. Fredriksson, H.; Hillert, M.; Lange, N. The modification of aluminium-silicon alloys by sodium. *J. Inst. Met.* **1973**, *101*, 285–299.
4. Flood, S.C.; Hunt, J.D. Modification of Al-Si eutectic alloys with Na. *Met. Sci.* **1981**, *15*, 287–294. [CrossRef]
5. Liu, Q.Y.; Li, Q.C.; Liu, Q.F. Modification of aluminum-silicon alloys with sodium. *Acta Metall. Mater.* **1991**, *39*, 2497–2502.
6. Hegde, S.; Prabhu, K.N. Modification of eutectic silicon in Al–Si alloys. *J. Mater. Sci.* **2008**, *43*, 3009–3027. [CrossRef]
7. Moniri, S.; Shahani, A.J. Chemical modification of degenerate eutectics: A review of recent advances and current issues. *J. Mater. Res.* **2019**, *34*, 20–34. [CrossRef]
8. Ashtari, P.; Tezuka, H.; Sato, T. Modification of Fe-containing intermetallic compounds by K addition to Fe-rich AA319 aluminum alloys. *Scr. Mater.* **2005**, *53*, 937–942. [CrossRef]
9. Jenkinson, D.C.; Hogan, L.M. The modification of aluminium-silicon alloys with strontium. *J. Cryst. Growth* **1975**, *28*, 171–187. [CrossRef]
10. Dahle, A.K.; Nogita, K.; McDonald, S.D.; Dinnis, C.; Lu, L. Eutectic modification and microstructure development in Al-Si Alloys. *Mater. Sci. Eng. A* **2005**, *413–414*, 243–248. [CrossRef]
11. Fracchia, E.; Gobber, F.S.; Rosso, M. Effect of Alloying Elements on the Sr Modification of Al-Si Cast Alloys. *Metals* **2021**, *11*, 342. [CrossRef]
12. Knuutinen, A.; Nogita, K.; McDonald, S.D.; Dahle, A.K. Modification of Al-Si alloys with Ba, Ca, Y and Yb. *J. Light Met.* **2001**, *1*, 229–240. [CrossRef]
13. Rao, J.; Zhang, J.; Liu, R.; Zheng, J.; Yin, D. Modification of eutectic Si and the microstructure in an Al-7Si alloy with barium addition. *Mater. Sci. Eng. A* **2018**, *728*, 72–79. [CrossRef]
14. Shlyaptseva, A.D.; Petrov, I.A.; Ryakhovsky, A.P.; Medvedeva, E.V.; Tcherdyntsev, V.V. Complex structure modification and improvement of properties of aluminium casting alloys with various silicon content. *Metals* **2021**, *11*, 1946. [CrossRef]
15. Sreeja Kumari, S.S.; Pillai, R.M.; Pai, B.C. Structure and properties of calcium and strontium treated Al–7Si–0.3Mg alloy: A comparison. *J. Alloys Compd.* **2008**, *460*, 472–477.
16. Abdollahi, A.; Gruzleski, J.E. An evaluation of calcium as a eutectic modifier in A357 alloy. *Int. J. Cast Met. Res.* **1998**, *11*, 145–155. [CrossRef]
17. Li, B.; Wang, H.; Jie, J.; Wei, Z. Effects of yttrium and heat treatment on the microstructure and tensile properties of Al–7.5Si–0.5Mg alloy. *Mater. Des.* **2011**, *32*, 1617–1622. [CrossRef]
18. Tsai, Y.C.; Chou, C.Y.; Lee, S.L.; Lin, C.K.; Lin, J.C.; Lim, S.W. Effect of trace La addition on the microstructures and mechanical properties of A356 (Al-7Si-0.35Mg) aluminum alloys. *J. Alloys Compd.* **2009**, *487*, 157–162. [CrossRef]
19. Tsai, Y.C.; Lee, S.L.; Lin, C.K. Effect of trace Ce addition on the microstructures and mechanical properties of A356 (AL-7SI-0.35Mg) aluminum alloys. *J. Chin. Inst. Eng.* **2011**, *34*, 609–616. [CrossRef]
20. Qiu, H.; Yan, H.; Hu, Z. Effect of samarium (Sm) addition on the microstructures and mechanical properties of Al–7Si–0.7Mg alloys. *J. Alloys Compd.* **2013**, *567*, 77–81. [CrossRef]
21. Li, J.H.; Wang, X.D.; Ludwig, T.H.; Tsunekawa, Y.; Arnberg, L.; Jiang, J.Z.; Schumacher, P. Modification of eutectic Si in Al–Si alloys with Eu addition. *Acta Mater.* **2015**, *84*, 153–163. [CrossRef]

22. Wang, Q.; Shi, Z.; Li, H.; Lin, Y.; Li, N.; Gong, T.; Zhang, R.; Liu, H. Effects of Holmium Additions on Microstructure and Properties of A356 Aluminum Alloys. *Metals* **2018**, *8*, 849. [CrossRef]

23. Shi, Z.M.; Wang, Q.; Zhao, G.; Zhang, R.Y. Effects of erbium modification on the microstructure and mechanical properties of A356 aluminum alloys. *Mater. Sci. Eng. A* **2015**, *626*, 102–107. [CrossRef]

24. Nogita, K.; McDonald, S.D.; Dahle, A.K. Eutectic modification of Al-Si alloys with rare earth metals. *Mater. Trans.* **2004**, *45*, 323–326. [CrossRef]

25. Li, J.H.; Suetsugu, S.; Tsunekawa, Y.; Schumacher, P. Refinement of eutectic Si phase in Al-5Si alloys with Yb additions. *Metall. Mater. Trans. A* **2012**, *44*, 669–681. [CrossRef]

26. Edwards, J.D.; Archer, R.S. The new aluminum-silicon alloys—An important process of "modification" and the remarkable improvement in properties it brings about. *Chem. Metall. Eng.* **1924**, *31*, 504–508.

27. Day, M.G.; Hellawell, A. The microstructure and crystallography of aluminium silicon eutectic alloys. *Proc. Royal Soc. A Math. Phys. Eng. Sci.* **1968**, *305*, 473–491.

28. Lu, S.; Hellawell, A. The mechanism of silicon modification in aluminum-silicon alloys: Impurity induced twinning. *Metall. Trans. A.* **1987**, *18*, 1721–1733.

29. Haynes, W.M.; Lide, D.R. (Eds.) *CRC Handbook of Chemistry and Physics*, 95th ed.; CRC Press: Boca Raton, FL, USA, 2014.

30. Gale, W.F.; Totemeier, T.C. (Eds.) *Smithells Metals Reference Book*, 8th ed.; Totemeier Imprint: Oxford, UK, 2003; p. 2080.

31. Altman, M.B.; Stromskaya, N.P.; Guskova, N.V. Method of Simultaneous Refining and Modification of Silumins. Patent SU 423867 A1, 15 April 1974.

32. Merkus, H.G. *Particle Size Measurements: Fundamentals, Practice, Quality*; Springer: Berlin/Heidelberg, Germany, 2009; 534p.

33. *ISO 10049:2019(E)*; Aluminium alloy castings—Visual method for assessing porosity. International Organization for Standardization: Geneva, Switzerland, 2019.

34. Stern, K.H. high temperature properties and decomposition of inorganic salts part 3, nitrates and nitrites. *J. Phys. Chem. Ref. Data* **1972**, *1*, 747–772. [CrossRef]

35. Gurevich, V.L.; Veyts, I.V. *Thermodynamic Properties of Individual Substances: A Handbook*; Nauka: Moscow, Russia, 1978; Volume 4.

36. Shin, S.S.; Kim, E.S.; Yeom, G.Y.; Lee, J.C. Modification effect of Sr on the microstructures and mechanical properties of Al–10.5Si–2.0Cu recycled alloy for die casting. *Mater. Sci. Eng. A* **2012**, *532*, 151. [CrossRef]

37. Hogan, L.M.; Song, H. Interparticle spacings and undercoolings in Al-Si eutectic microstructures. *Met. Trans. A* **1987**, *18*, 707–713. [CrossRef]

38. Nogita, K.; Yasuda, H.; Yoshiya, M.; McDonald, S.D.; Uesugi, K.; Takeuchi, A.; Suzuki, Y. The role of trace element segregation in the eutectic modification of hypoeutectic Al–Si alloys. *J. Alloys. Compd.* **2010**, *489*, 415–420. [CrossRef]

39. Sigworth, G.K. Modification of Aluminum-Silicon Alloys, Casting. In *ASM Handbook*; Viswanathan, S., Apelian, D., Donahue, R.J., DasGupta, B., Gywn, M., Jorstad, J.L., Monroe, R.W., Sahoo, M., Prucha, T.E., Twarog, D., Eds.; ASM International: Detroit, MI, USA, 2008; pp. 240–254. [CrossRef]

40. Ardo, D. Porosity in aluminum foundry alloys—The effect of modification. In Proceedings of the International Symposium on Reduction and Casting of Aluminum, Montreal, QC, Canada, 28–31 August 1988; Ardo, D., Gruzleski, J.E., Eds.; Pergamon Press: Oxford, UK, 1988; pp. 263–282.

41. Andrushevich, A.A.; Sadokha, M.A. Shrinkage phenomena in silumins when treated with long-acting modifiers. *Foundry Prod. Metall.* **2022**, *3*, 30–35. [CrossRef]

42. Nogita, K.; McDonald, S.D.; Zindel, J.W.; Dahle, A.K. Eutectic solidification mode in sodium modified Al-7 mass%Si-3.5 mass%Cu-0.2 mass%Mg casting alloys. *Mater. Trans.* **2001**, *42*, 1981–1986. [CrossRef]

43. Knuutinen, A.; Nogita, K.; McDonald, S.S.; Dahle, A.K. Porosity formation in aluminium alloy A356 modified with Ba, Ca, Y and Yb. *J. Light Met.* **2001**, *1*, 241–249. [CrossRef]

44. Huang, C.; Liu, Z.; Li, J. Influence of Alloying Element Mg on Na and Sr Modifying Al-7Si Hypoeutectic Alloy. *Materials* **2022**, *15*, 1537. [CrossRef]

45. Ganesh, M.S.; Reghunath, N.; Levin, M.J.; Prasad, A.; Doondi, S.; Shankar, K.V. Strontium in Al–Si–Mg Alloy: A Review. *Met. Mater. Int.* **2022**, *28*, 1–40. [CrossRef]